

NANO EXPRESS

Open Access

Distribution of Nd³⁺ ions in oxyfluoride glass ceramics

Hua Yu¹, Hui Guo¹, Ming Zhang¹, Yan Liu¹, Min Liu¹ and Li-juan Zhao^{1,2*}

Abstract

It has been an open question whether Nd³⁺ ions are incorporated into the crystalline phase in oxyfluoride glass ceramics or not. Moreover, relative research has indicated that spectra characters display minor differences between before and after heat treatment in oxyfluoride glass compared to similar Er³⁺-, Yb³⁺-, Tm³⁺-, Eu³⁺-, etc.-doped materials. Here, we have studied the distribution of Nd³⁺ ions in oxyfluoride glass ceramics by X-ray diffraction quantitative analysis and found that almost none of the Nd³⁺ ions can be incorporated into the crystalline phase. In order to confirm the rationality of the process, the conventional mathematical calculation and energy-dispersive spectrometry line scanning are employed, which show good consistency. The distribution of Nd³⁺ ions in oxyfluoride glass ceramics reported here is significant for further optical investigations and applications of rare-earth doped oxyfluoride glass ceramics.

Keywords: Nd, Glass ceramics, Nanocrystal, Distribution

Background

Nd³⁺ is always considered to be one of the most efficient rare-earth (RE) ions to generate laser operation around 1.06 μm in different hosts, such as crystals and glasses. In the 1970s, transparent glass ceramics (GCs) with nanocrystals (NCs) of about 50 nm were originally suggested to be used as laser host materials [1,2]. In subsequent oxide glass system studies, the fluorescence lifetimes and absorption spectra of Nd³⁺ ions were measured in neodymium-doped glasses and GCs to investigate the distribution of the Nd³⁺ ions [3]. The results indicated that Nd³⁺ ions were excluded from the crystalline phase and accumulated into the residual glass matrix in the GCs. Also, in a similar glass system, Dymnikov et al. [4] and Kang et al. [5], respectively, found that Nd³⁺ ions exhibited fairly different distribution tendencies when the crystalline phase varied in glass ceramics by performing fluorescence, absorption, and Judd-Ofelt analyses.

In 1993, Wang and Ohwaki, for the first time, reported the fabrication of transparent oxyfluoride GCs which combined the advantages of fluoride glasses with efficient frequency upconversion and oxide glasses with good

chemical and mechanical stability [6]. RE ions, specifically Er³⁺ and Yb³⁺ ions, could be dissolved into the crystalline phase with lower phonon energy, generating a remarkable increase of luminescence, which made the transparent GCs potential outstanding laser host materials. Afterwards, extensive studies on RE-doped (Er\Eu\Yb\Ho) oxyfluoride GCs were carried out with various compositions and proportions [7-9]. Nevertheless, fewer studies were performed on Nd³⁺-doped oxyfluoride GCs, different from Er³⁺\Yb³⁺\Tm³⁺\Eu³⁺ ions, as Nd³⁺ ions were found to be difficultly incorporated into the crystalline phase [5,10-12]. Pisarska et al. [10,11] revealed that in oxyfluoroborate glass compositions, the ⁴F_{3/2} fluorescence lifetime didn't change after thermal treatment, showing that Nd³⁺ ions did not incorporate into the crystalline phase. Abril et al. [13] focused on different preparation methods with various Nd³⁺ ions sources and the corresponding distributions of Nd³⁺ ions in GCs. NdF₃ was thought to be more helpful for Nd³⁺ ions to be incorporated into the crystalline phase using analysis of fluorescence, absorption, and the Judd-Ofelt theory [13,14]. From the previous research mentioned above, whether in the Nd³⁺-doped oxide glass system, oxyfluoroborate glass compositions, or similar oxyfluoride glass system, Nd³⁺ ions were difficultly incorporated into the crystalline phase, while Wang et al. [15-18] investigated the thermal and optical properties of different

* Correspondence: zhaolj@nankai.edu.cn

¹The Key Laboratory of Weak-Light Nonlinear Photonics, Ministry of Education, School of Physics, Nankai University, Tianjin 300071, China

²Applied Physics School of TEDA, Nankai University, Tianjin 300457, China

kinds of Nd³⁺-doped GCs, which suggested that most of Nd³⁺ ions were doped in the crystalline phase.

While most of the previous research focused on incorporating the RE ions into the nanocrystals, such as Er³⁺\Yb³⁺\Tm³⁺\Eu³⁺ ions, the distribution of Nd³⁺ ions in GCs is somewhat ambiguous and exhibits some peculiar results, which much influences the materials' fluorescence properties. As previously reported about the distribution of Nd³⁺ in various oxyfluoride glass ceramics, indirect characterization techniques, for example, fluorescence analysis, X-ray diffraction (XRD), Judd-Ofelt theory calculation, and the like, were used. The properties of samples doped with Nd³⁺ ions show small changes after thermal treatment. Even with the slight changes caused by the distribution of Nd³⁺ ions in the nanocrystalline phase or glass phase, the Nd³⁺ ion segregation in the glass matrix also leads to the same results, that is to say that most of the results obtained from the indirect characterization technique cannot distinguish between Nd³⁺ ions entering into the nanocrystalline phase and locating on the interface between the crystalline and glassy phase. Nowadays, direct characterization technique energy dispersive X-ray spectroscopy (EDS, conventional fixed point measurement) was used to study the distribution of Nd³⁺ ions in glass ceramics. Since the crystal size is smaller than the probe beam, the analyzed volume in GC always includes both crystalline and glassy phases; the results of EDS do not seem to be entirely reliable.

In this paper, a direct and quantitative investigation on the distribution of Nd³⁺ ions in GCs was performed. Transparent GCs doped with Nd³⁺ ions were prepared, and subsequently, the glass matrix was etched off for releasing the fluoride nanoparticles (NPs) into the water phase for further study. In contrast, investigating the EDS of NPs rather than that of GCs is a more scientific and more convenient method to obtain the chemical composition of NP. The Nd³⁺ ion distribution model was built in GCs and NPs. EDS line scan by high-angle annular dark-field scanning transmission electron microscopy (HAADF-STEM) on the concentrations of concerned elements and the Rietveld full-pattern fitting algorithm were employed for quantitatively clarifying the distribution of Nd³⁺ ions in GCs. The results will be of great significance for the RE distribution investigations and further applications of Nd³⁺-doped glass ceramics.

Methods

Precursor glasses (PGs) with the composition of 44SiO₂-5Al₂O₃-40PbF₂-10CdF₂-1NdF₃ (mole ratio) were fabricated with a traditional melting-quenching route. Transparent GCs were obtained by following thermal treatment at 440 °C under the guidance of differential scanning calorimetry result of as-quenched precursor samples. The GCs were then ground into powder, immersed into

hydrofluoric acid solutions, and stirred with a magnetic stirrer so as to thoroughly release the nanocrystals from the glass matrix. Afterwards, nanocrystal powder was obtained by vacuum drying at 80 °C. This fabrication method has been reported in detail in the previous work [19].

All XRD data were obtained with a Rigaku D/Max-2500 diffractometer (Rigaku Corporation, Tokyo, Japan), using CuK α as the radiation. Quantitative analysis of the phases in NCs was carried out with material analysis using diffraction (MAUD) program (Luca Lutterotti, University of Trento, Trento, Italy) [20,21] applying the RITA/RISTA method based on the Rietveld full-pattern fitting algorithm with XRD data in the range of 10° to 125° acquired in step-scan mode with a step of 0.02° (2θ) at a counting time of 1 s per step. The program was developed to analyze diffraction spectra and obtain crystal structures, quantity, and microstructure of phases along with the texture and residual stresses. High-resolution transmission electron microscope (HRTEM) analysis was performed to observe the morphology of samples on a Philips TZOST TEM (FEI Co., Hillsboro, OR, USA) operating at 200 kV. STEM and EDS line scan were performed on a Tecnai G2F30 field-emission transmission electron microscope (FE-TEM; FEI Co., Hillsboro, OR, USA) using HAADF as imaging mode. All the measurements proceeded under the same condition.

Results and discussion

Figure 1a shows the diffraction patterns of compounds of GCs, along with the diffraction pattern of PGs without thermal treatment. Two curves show an overlap of the peaks corresponding to the amorphous matrix of the Si-Al glass. The differences between PGs and GCs indicate that the crystallization process takes place in the glass matrix under thermal treatment, and the characteristic diffraction peaks of pure cubic β-PbF₂ (JCPDS: 06-0251) emerge. XRD patterns of the GCs were compared with the theoretical calculation by program Diamond 3.1day (Crystal Impact GbR, Bonn, Germany) based on the structure of pure cubic β-PbF₂. Since the calculation results can only be expressed in the form of a vertical bar theoretically (see vertical bars in Figure 1c), the XRD trace (raw data) was converted to the form of integral intensities of peaks (i.e., the peak area value, see vertical bars in Figure 1b) in order to compare with the theoretical results. Indexing was also taken as exhibited in Figure 1b, c. As seen in Figure 1b,c, the positions and integral intensities of the peaks derived from the experiment are very consistent with the calculation based on the structure of pure cubic β-PbF₂. Quantitative calculation indicates that the average relative errors between the theoretical and experimental values are only 0.98% and 4.37% in 2θ and the relative intensity for every peak, respectively. In order to

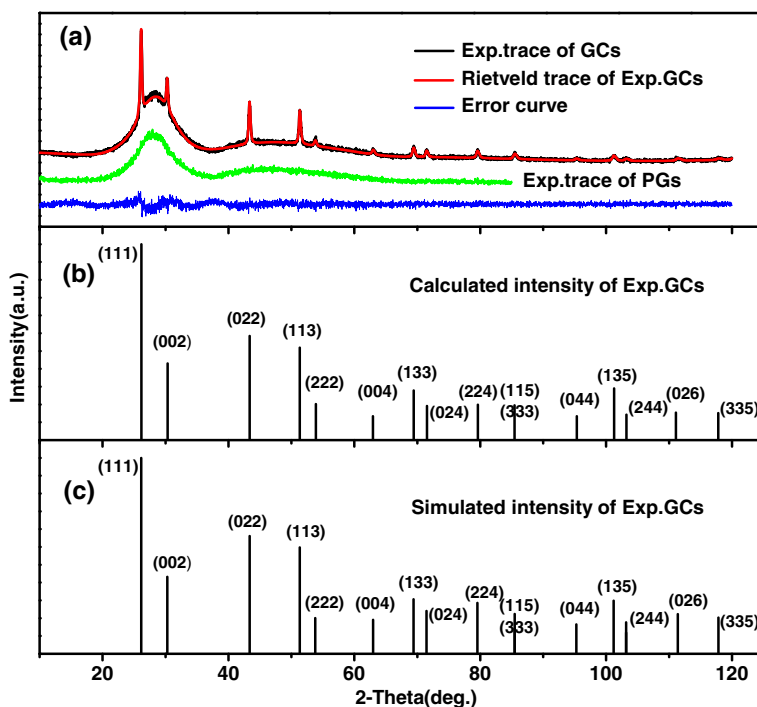


Figure 1 X-ray diffraction patterns of GCs and PGs. (a) Rietveld analyses for XRD pattern of GCs and the error curve. (b) The calculated line spectrum from peak area of GCs and (c) the simulated line spectrum of GCs from the Diamond program are presented for comparison.

further confirm the validity of the nanocrystal structure, pure cubic β -PbF₂, X-ray data refinement was made using the program MAUD. The analysis was started assuming the structure of β -PbF₂ ($F_{m\bar{3}m}$ no. 225) for the nanocrystal phase and the structure of cubic amorphous silica-Al glass (P_{213} no. 198) for the amorphous phase. The used crystalline structures can all be found in the database of the MAUD program. The corresponding factors R_{wp} (4.69%) and R_{exp} (4.27%) indicate a relatively good agreement between the experimental and calculated patterns. According to the results of the obtained quantitative analysis, about 8.6 mol% to 13.5 mol% of the original Pb would contribute to form crystalline β -PbF₂ during the thermal treatment. In addition, the structure cell parameter of the nanocrystal phase corresponds to that of the pure cubic β -PbF₂, which further checks the structure of the nanocrystal phase.

The Nd³⁺ ions could not be incorporated into the nanocrystal phase by the reason that the structure of the nanocrystal phase is pure cubic β -PbF₂. Corrosion-treated methods were applied to acquire the NCs so as to explore the information on chemical compositions and structures of nanocrystals and weaken the interference of the glass matrix. For Nd³⁺-doped samples, an unusual change happens when the nanocrystals embedded in the glass matrix abstracted by etching process. Unlike our previous work [22] of Er³⁺/Yb³⁺-codoped

GCs wherein only β -PbF₂ phase was observed, the complex mixture was obtained after etching off the glass matrix of GCs doped with Nd³⁺. With peak indexing, the additional intense diffraction peaks appear to be NdF₃ (JCPDS: 09-0416) and Pb₃AlF₉·H₂O (JCPDS: 45-1458) phases. The new crystal phase NdF₃ is generated in the course of the etching treatment, wherein Nd³⁺ ions existing in the glass matrix react with F⁻ ions in acid, generating NdF₃. Likewise, Pb and Al ions of the glass matrix reacting with F⁻ ions in acid generate the Pb₃AlF₉·H₂O phase. MAUD program based on the Rietveld method was used to calculate the relative amounts of β -PbF₂ and NdF₃ phases. The crystal structure information of the concerned phases is acquired from the Crystallography Open Database [23]. The refinement results and difference plot for the observed and calculated patterns of NPs are shown in Figure 2. The refining factors of R_{wp} (8.07%) and R_{exp} (4.02%) indicate a good agreement between the experimental and calculated patterns. The structure cell parameter of β -PbF₂ obtained from the refinement of NCs (0.5890 nm) and GCs (0.5898 nm) is nearly the same as that of pure β -PbF₂ (0.5927 nm), which further verifies the existence of Nd³⁺ outside the NCs. According to other relative results obtained from Rietveld analysis, the cell parameters of the other two phases are nearly the same as those of the standard structures separately, which further certifies the authenticity of the complex phases suggested

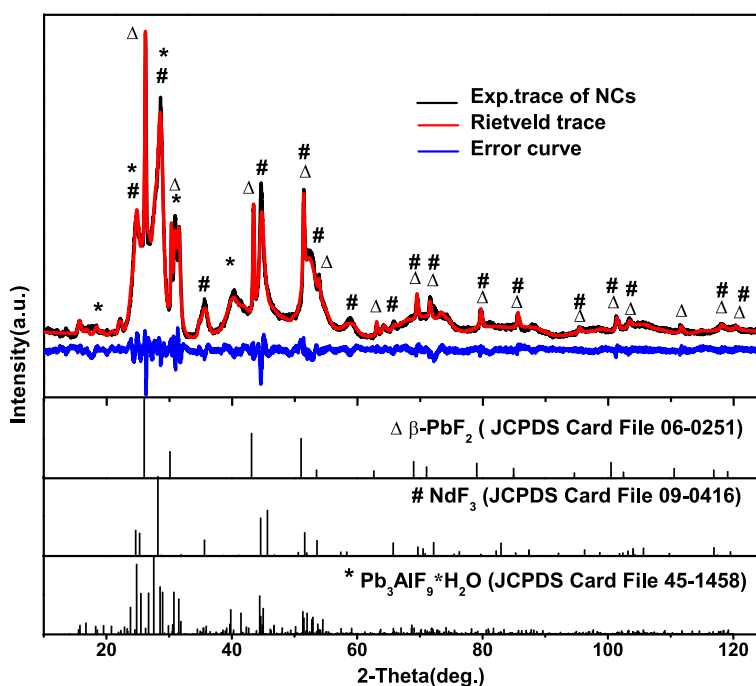


Figure 2 Rietveld analyses for XRD pattern of NCs and the error curve. The line spectrum of $\beta\text{-PbF}_2$, NdF_3 , and $\text{Pb}_3\text{AlF}_9\cdot\text{H}_2\text{O}$ are revealed for comparison.

above. From the results of the relative weight fraction obtained from refinement, moreover, through the sample arithmetic conversion, we can assume that about 10.9 mol % of the Pb of the raw material contribute to form the crystalline $\beta\text{-PbF}_2$ phase during the thermal treatment. This conclusion is in accordance with the Rietveld analysis data from Figure 1.

High-resolution TEM micrographs of GCs and NCs are displayed in Figure 3, providing a visual characterization of the samples and a direct analysis method. In GCs, as shown in Figure 3a, only spherical $\beta\text{-PbF}_2$ nanocrystals with an average size of about 22 nm distribute in the glass matrix, which has a good consistency with the calculated size using the Scherrer formula. However, in NCs, besides the 22-nm nanocrystals already existing in GCs, as shown in Figure 3b, a large amount of additional crystals and flake-like substrates also emerges. Particularly, most of these additional crystals assemble around the known $\beta\text{-PbF}_2$ nanocrystals, forming a core-shell-like structure. According to the HRTEM micrographs, the periodic arrayed crystal planes can be viewed clearly, and a part of symbolic interplanar distance (d) values, which were measured accurately for both GC and NCs, has been labeled. The measured values of d , 0.294 or 0.295 nm for Figure 3a,b, are attributed to the crystal plane (002) of pure cubic $\beta\text{-PbF}_2$ as the core, while the d values of 0.303 and 0.316 nm around the $\beta\text{-PbF}_2$ nanocrystal belong to crystal planes (020) and (-121) of the shell NdF_3 , respectively, and the other one d value of 1.141 nm is for the

symbolic crystal plane (001) of the substrates $\text{Pb}_3\text{AlF}_9\cdot\text{H}_2\text{O}$. This conclusion is in accordance with the XRD refinement result of NCs, which has been displayed in Figure 2 above. On the basis of Rietveld refining results and HRTEM micrographs, the Nd^{3+} ions are reserved in the glass matrix after thermal treatment and aggregated outside $\beta\text{-PbF}_2$ particles in the form of NdF_3 crystals when the glass matrix is removed through the etching process. Therefore, a simplified model is proposed to describe the distribution of Nd^{3+} ions both in GCs and NCs, as shown in the insets of Figure 3a,b. That is to say, with thermal treatment on PGs, the phase segregation process happens, and on the one hand, as shown in the inset of Figure 3a, Nd^{3+} ions with a nonhomogeneous distribution form an aggregate structure, which has been reported on the previous research [13,14]; on the other hand, Pb and F elements get together to form high-temperature phase $\beta\text{-PbF}_2$ nanocrystals, while the formation of Nd^{3+} clusters prevents the process of incorporation into the $\beta\text{-PbF}_2$ phase. During the etching process for removing the glass matrix, the Nd^{3+} ions meet F^- ions in the acid solution and generate NdF_3 crystals. Then, the large quantities of NdF_3 crystals adsorb the surface of the $\beta\text{-PbF}_2$ nanoparticles. The model for NCs is simplified as a core-shell structure for further analysis, *viz.*, the $\beta\text{-PbF}_2$ particle as the core and the covering NdF_3 crystals as the shell, as shown in the inset of Figure 3b. This rough simplification is acceptable considering the quantitative analysis result of NCs.

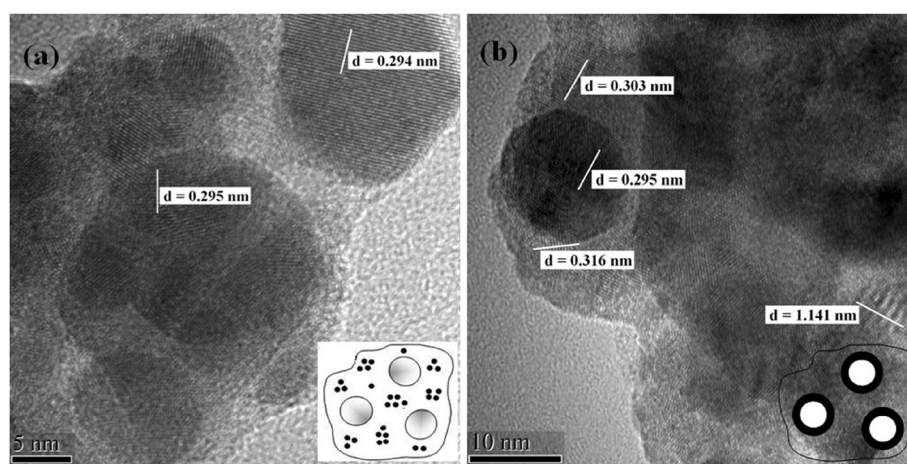


Figure 3 High-resolution TEM micrographs with marked interplanar distance d values of (a) GCs and (b) NCs. The insets are the simplified models for GCs and NCs, where the large white spheres stand for $\beta\text{-PbF}_2$ nanocrystals, and small black spheres in GCs are for Nd^{3+} ions.

In order to verify the anticipation, EDS line scans in HAADF mode across the $\beta\text{-PbF}_2$ particles are carried out on a Tecnai G2F30 FE-TEM to offer signal intensity values for different elements. The line scanning paths are shown in Figure 4a,b, and the results are shown in Figure 4e,f. In GCs, the detected trace of Nd in EDS like that of Cd indicates that the nanocrystalline phase is pure $\beta\text{-PbF}_2$, rather than $\beta\text{-PbF}_2\text{:RE}$, as previously suggested by many researchers. Even the trace of Nd in EDS of the other samples doped with different concentrations of Nd, the former researches confirmed that Cd hardly congregated in the nanocrystals, which also indicated that none of the Nd ions were incorporated into the $\beta\text{-PbF}_2$ crystalline phase [22,24,25]. Figure 4c shows the EDS line scan for the ideal spheric body model of crystalline $\beta\text{-PbF}_2$ in GCs. As an ideal sphere model, dot A is for the center of it. Axial direction (Z) is the orientation of the EDS line scan. Dot O and length x are the initial point and the distance of the line scan separately. From Figure 4c, we can get that from the relation formula, the content of Pb satisfies

$$Y_1 \propto 2\sqrt{R^2 - (R - x)^2} \quad (1)$$

where Y_1 is the relative intensity of element Pb, R is the half size of the $\beta\text{-PbF}_2$ nanocrystal, and x is the length of the line scan. Through conventional mathematical analysis, the simulated curve is shown in Figure 4e, which is in accordance with the fitting curve of the experimental measurement. In the same way, the ideal core-shell structure model of NCs, which is shown in Figure 4d, is analyzed by conventional mathematical simulation, as shown in Figure 4f. From Figure 4d, the signal intensity ratio of the content of Pb and Nd can be

expressed by the following formula:

$$Y_2 \propto \frac{\sqrt{R_2^2 - (R_2 - x)^2}}{\sqrt{R_1^2 - (R_2 - x)^2} - \sqrt{R_2^2 - (R_2 - x)^2}} \quad (2)$$

where Y_2 is the relative element intensity ratio Pb/Nd, R_1 and R_2 are the half sizes of the core-shell model and $\beta\text{-PbF}_2$ nanocrystal respectively, and x is the length of the line scan. The accordance with experimental results, as shown in Figure 4e,f, proves the rationality of the model. Therefore, it is concluded that all of the Nd^{3+} ions are located in the glass matrix, while few of the Nd^{3+} ions dope into crystalline phase.

As a result from that, due to Nd^{3+} ions aggregating into the glass matrix rather than incorporating into the $\beta\text{-PbF}_2$ crystalline phase during thermal treatment, Nd^{3+} ion-doped oxyfluoride glass exhibits a weak difference in fluorescence and other optical properties before and after heat treatment. On one hand, the location of Nd^{3+} ions is the oxide environment with a higher coupled phonon energy, which will boost nonradiative relaxation process, compared with fluoride nanocrystal phase; on the other hand, aggregation of Nd^{3+} ions can also bring some much smaller effects on fluorescence and optical properties than that of GCs doped with Nd^{3+} ions into the fluoride nanocrystal phase. This is in agreement with some previous research, such as what was discussed by Rapp et al. in [3]; the fluorescence lifetimes of Nd^{3+} ions were much shorter than those in glasses, and the absorption and emission spectra of Nd^{3+} ions were identical both in neodymium-doped glasses and GCs, which indicated that neodymium ions were excluded from the crystalline phase of GCs and were entirely accumulated in

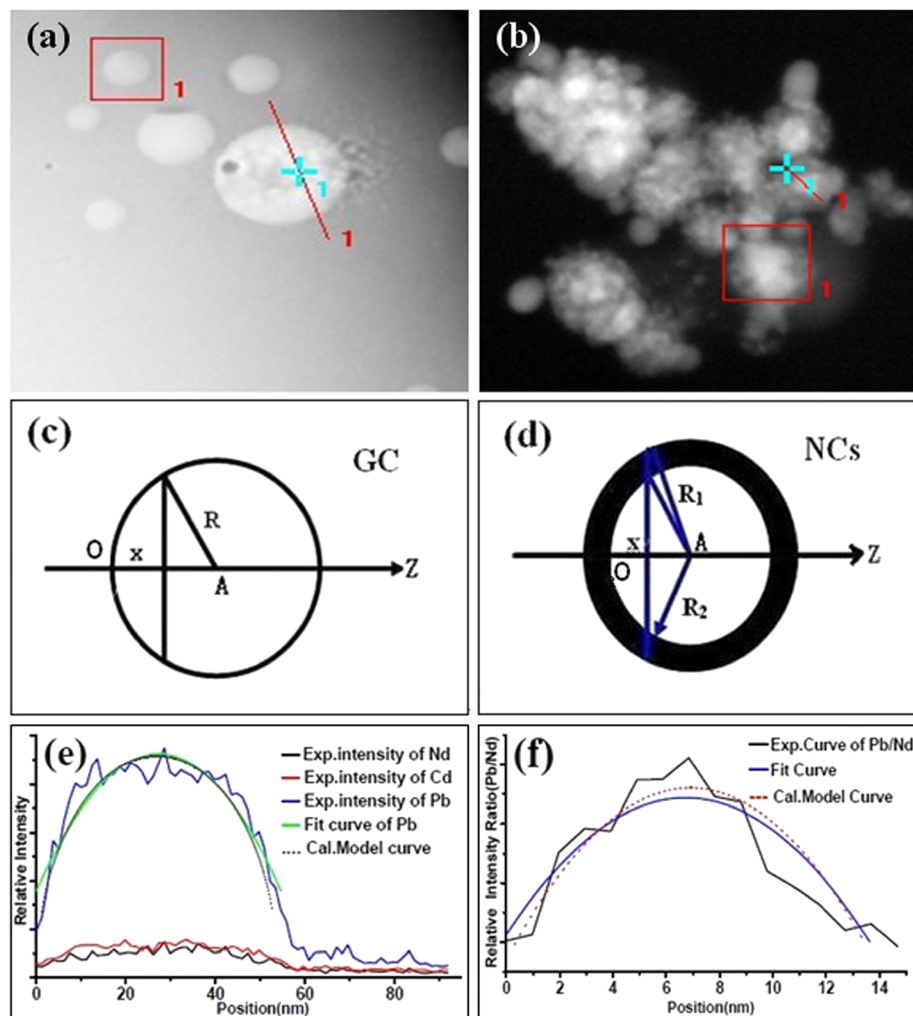


Figure 4 EDS line scan graphs in HAADF mode (a,b). EDS line scans for the ideal models of (c) crystalline $\beta\text{-PbF}_2$ and (d) core-shell structure in NCs. (e) The relative element signal intensity of Pb, Nd, and Cd in GC; the fit curve; and the calculated model curve of element Pb are presented for comparison; (f) The fit curve of relative element intensity ratio Pb/Nd in NCs and the calculated core-shell model curve are also shown.

the glass matrix. However, the most noteworthy thing is that the segregation of Nd^{3+} ions in the glass matrix also leads to the same results; in other words, most of the results obtained from indirect characterization techniques cannot distinguish between Nd^{3+} ions entering into the crystalline phase and locating on the interface between the crystalline and glassy phase. Therefore, unlike those indirect characterization techniques used by most of previous research, a direct and quantitative investigation method was employed to present a clear result that almost none of the Nd^{3+} ions can be incorporated into the crystalline phase but reside in the glass matrix.

Conclusions

Transparent Nd^{3+} -doped GCs were prepared and corrosion-treated to release NCs from the glass matrix for a direct study on their composition and structure

information. Unlike the former results, $\beta\text{-PbF}_2:\text{RE}$ crystalline phase was obtained, and pure $\beta\text{-PbF}_2$ crystalline phase was generated after thermal treatment. Especially after etching off the glass matrix, massive NdF_3 crystals simultaneously generate in free NCs. Through the XRD Rietveld refining method, almost the whole of Nd^{3+} ions reside in the glass matrix despite that the samples undergo the thermal treatment. For further demonstration, the models of Nd^{3+} ions existing in the glass matrix in GCs and the core-shell-like structure of pure $\beta\text{-PbF}_2$ surface absorbing NdF_3 crystals in NCs were built. Then, HRTEM, EDS line scan in HAADF mode, and conventional mathematical analysis were used to verify the models' rationality. The results of experimental characterization well coincide with those of the simulation. Our work explains the previous arguments about whether Nd^{3+} ions doped into the crystalline phase or not and removes the

puzzle about minor differences on spectral properties. The study has paved a way to more comprehensively understand the properties of the Nd³⁺-doped oxyfluoride glass. The results here would benefit further research on the optical properties and applications of such materials.

Competing interests

The authors declare that they have no competing interests.

Acknowledgments

The authors would like to acknowledge the financial support of the Key Natural Scientific Foundation of Tianjin under Grant No. 9JCZDJC16700 and the Fundamental Research Funds for the Central Universities. The authors are also grateful to the doctoral candidate Nan Hu who is studying in the Institute of Physical Chemistry, Johannes Gutenberg-Universität Mainz for his enthusiastic help and kind guidance.

Authors' contributions

LjZ and HY conceived the total study and wrote the manuscript. HG and MZ were involved in the experiments and Rietveld analysis. YL and ML participated in the analysis of HRTEM and EDS. All authors read and approved the final manuscript.

Authors' information

LjZ is a professor in the School of Physics and TEDA Applied Physics School of Nankai University. HY is an associate professor in the School of Physics. HG, MZ, and YL are master students. ML is a doctoral candidate.

Received: 16 April 2012 Accepted: 18 May 2012

Published: 30 May 2012

References

- Müller G: Glass ceramic-a new laser host material. *J Appl Phys* 1972, **44**:2315–2318.
- Rapp CF, Chrysochoos J: Neodymium-doped glass-ceramic laser material. *J Mater Sci* 1972, **7**:1090–1092.
- Rapp CF, Chrysochoos J: Fluorescence lifetimes of neodymium-doped glasses and glass-ceramics. *J Phys Chem* 1973, **77**:1016–1018.
- Dymnikov AA, Dymshits OS, Zhilin AA, Savostjanov VA, Chuvaeva TI: The structure of luminescence centers of neodymium in glasses and transparent glass-ceramics of the Li₂O-Al₂O₃-SiO₂ system. *J Non-Cryst Solids* 1996, **196**:67–72.
- Kang U, Chuvaeva TI, Onushchenko AA, Shashkin AV, Zhilin AA, Kim H-J, Chang Y-G: Radiative properties of Nd-doped transparent glass-ceramics in the lithium aluminosilicate system. *J Non-Cryst Solids* 2000, **278**:75–84.
- Wang Y, Ohwaki J: New transparent vitroceramics codoped with Er³⁺ and Yb³⁺ for efficient frequency upconversion. *Appl Phys Lett* 1993, **63**:3268–3270.
- Beggiora M, Reaney IM, Islam MS: Structure of the nanocrystals in oxyfluoride glass ceramics. *Appl Phys Lett* 2003, **83**:467–469.
- Dejneca MJ: The luminescence and structure of novel transparent oxyfluoride glass-ceramics. *J Non-Cryst Solids* 1998, **239**:149–155.
- Pan JJ, Xu RR, Tian Y, Li KF, Hu LL, Zhang JJ: 2.0 μm emission properties of transparent oxyfluoride glass ceramics doped with Yb³⁺-Ho³⁺ ions. *Opt Mater* 2010, **32**:1451–1455.
- Pisarska J, Ryba-Romanowski W, Dominiak-Dzik G, Goryczka T, Pisarski WA: Nd-doped oxyfluoroborate glasses and glass-ceramics for NIR laser applications. *J Alloys Compd* 2008, **451**:223–225.
- Pisarska J, Ryba-Romanowski W, Dominiak-Dzik G, Goryczka T, Pisarski WA: Near-infrared luminescence of rare earth ions in oxyfluoride lead borate glasses and transparent glass-ceramic materials. *Opt Appl* 2008, **38**:211–216.
- Abrial M, Mendez-Ramos J, Martin IR, Rodriguez-Mendoza UR, Lavin V, Delgado-Torres A, Rodriguez VD, Nunez P, Lozano-Gorrin AD: Optical properties of Nd³⁺ ions in oxyfluoride glasses and glass ceramics comparing different preparation methods. *J Appl Phys* 2004, **95**:5271–5279.
- Lavin V, Iparraguirre I, Azkargorta J, Mendioroz A, Gonzalez-Platas J, Balda R, Fernandez J: Stimulated and upconverted emissions of Nd³⁺ in a transparent oxyfluoride glass-ceramic. *Opt Mater* 2004, **25**:201–208.
- Mendez-Ramos J, Abril M, Martin IR, Rodriguez-Mendoza UR, Lavin V, Rodriguez VD, Nunez P, Lozano-Gorrin AD: Ultraviolet and visible upconversion luminescence in Nd³⁺-doped oxyfluoride glasses and glass ceramics obtained by different preparation methods. *J Appl Phys* 2006, **99**(1–5):113510.
- Chen DQ, Wang YS, Yu YL, Hu ZJ: Crystallization and fluorescence properties of Nd³⁺-doped transparent oxyfluoride glass ceramics. *Mater Sci Eng B* 2005, **123**:1–6.
- Yu YL, Chen DQ, Cheng Y, Wang YS, Hu ZJ, Bao F: Investigation on crystallization and influence of Nd³⁺ doping of transparent oxyfluoride glass-ceramics. *J Eur Ceram Soc* 2006, **26**:2761–2767.
- Liu F, Wang YS, Chen DQ, Yu YL: Investigation on crystallization kinetics and microstructure of novel transparent glass ceramics containing Nd: NaYF₄ nano-crystals. *Mater Sci Eng B* 2007, **136**:1006–1010.
- Chen DQ, Wang YS, Ma E, Yu YL, Liu F, Li RF: Spectroscopic and stimulated emission characteristics of Nd³⁺ in transparent glass ceramic embedding β-YF₃ nanocrystals. *J Appl Phys* 2007, **102**(1–6):023504.
- Yu H, Hu N, Wang YN, Wang ZL, Gan ZS, Zhao LJ: The fabrication of nanoparticles in aqueous solution from oxyfluoride glass ceramics by thermal induction and corrosion treatment. *Nanoscale Res Lett* 2008, **3**:516–520.
- Wend HR, Matthies S, Lutterotti L: Texture analysis from diffraction spectra. *Mat Sci Forum* 1994, **157**–162:473–480.
- Ferrari M, Lutterotti L: Method for the simultaneous determination of anisotropic residual stresses and texture by X-ray diffraction. *J Appl Phys* 1994, **76**:7246–7255.
- Hu N, Yu H, Zhang M, Zhang P, Wang YZ, Zhao LJ: The tetragonal structure of nanocrystals in rare-earth doped oxyfluoride glass ceramics. *Phys Chem Chem Phys* 2011, **13**:1499–1505.
- Crystallography Open Database. <http://www.crystallography.net/>.
- Tikhomirov VK, Mortier M, Gredin P, Patriarche G, Gorller-Walrand C, Moschchalkov VV: Preparation and up-conversion luminescence of 8 nm rare-earth doped fluoride nanoparticles. *Opt Express* 2008, **16**:14544.
- Beggiora M, Reaney IM, Islam MS: Structure of the nanocrystals in oxyfluoride glass ceramics. *Appl Phys Lett* 2003, **83**:467.

doi:10.1186/1556-276X-7-275

Cite this article as: Yu et al.: Distribution of Nd³⁺ ions in oxyfluoride glass ceramics. *Nanoscale Research Letters* 2012 **7**:275.

Submit your manuscript to a SpringerOpen® journal and benefit from:

- Convenient online submission
- Rigorous peer review
- Immediate publication on acceptance
- Open access: articles freely available online
- High visibility within the field
- Retaining the copyright to your article

Submit your next manuscript at ► springeropen.com